Journal for ImmunoTherapy of Cancer

Combination oncolytic virus, radiation therapy, and immune checkpoint inhibitor treatment in anti-PD-1-refractory cancer

Sachin R Jhawar,[1] Shang-Jui Wang,[1] Aditya Thandoni,[2] Praveen K Bommareddy ,[3] Jenna H Newman,[3] Eileena F Giurini,[4] Amanda L Marzo,[4] Timothy M Kuzel,[4] Vineet Gupta,[4] Jochen Reiser,[4] Preston Daniels,[4] Devora Schiff,[3] Darrion Mitchell,[1] Nicole R LeBoeuf,[5,6] Christopher Simmons,[7] Sharad Goyal,[8] Ahmed Lasfar,[3,9] Jose A Guevara-Patino ,[10] Bruce G Haffty,[3] Howard L Kaufman ,[11] Ann W Silk ,[5,7] Andrew Zloza [4]

To cite: Jhawar SR, Wang S-J, Thandoni A, *et al*. Combination oncolytic virus, radiation therapy, and immune checkpoint inhibitor treatment in anti-PD-1-refractory cancer. *Journal for ImmunoTherapy of Cancer* 2023;**11**:e006780. doi:10.1136/jitc-2023-006780

► Additional supplemental material is published online only. To view, please visit the journal online (http://dx.doi.org/10.1136/jitc-2023-006780).

Accepted 16 June 2023

For numbered affiliations see end of article.

Correspondence to
Dr Ann W Silk;
ann_silk@dfci.harvard.edu

Dr Andrew Zloza;
andrewzloza@gmail.com

ABSTRACT

Background Immunotherapies are becoming front-line treatments for many advanced cancers, and combinations of two or more therapies are beginning to be investigated. Based on their individual antitumor capabilities, we sought to determine whether combination oncolytic virus (OV) and radiation therapy (RT) may improve cancer outcomes.

Methods To investigate the activity of this combination therapy, we used in vitro mouse and human cancer cell lines as well as a mouse model of skin cancer. After initial results, we further included immune checkpoint blockade, whose addition constituted a triple combination immunotherapy.

Results Our findings demonstrate that OV and RT reduce tumor growth via conversion of immunologically 'cold' tumors to 'hot', via a CD8+ T cell-dependent and IL-1α-dependent mechanism that is associated with increased PD-1/PD-L1 expression, and the triple combination of OV, RT, and PD-1 checkpoint inhibition impedes tumor growth and prolongs survival. Further, we describe the response of a PD-1-refractory patient with cutaneous squamous cell carcinoma who received the triple combination of OV, RT, and immune checkpoint inhibitor (ICI), and went on to experience unexpected, prolonged control and survival. He remains off-treatment and is without evidence of progression for >44 months since study entry.

Conclusions Effective systemic antitumor immune response is rarely elicited by a single therapy. In a skin cancer mouse model, we demonstrate improved outcomes with combination OV, RT, and ICI treatment, which is associated with mechanisms involving augmented CD8+ T cell infiltration and IL-1α expression. We report tumor reduction and prolonged survival of a patient with skin cancer treated with combination OV, RT, and ICI. Overall, our data provide strong rationale for combining OV, RT, and ICI for treatment of patients with ICI-refractory skin and potentially other cancers.

WHAT IS ALREADY KNOWN ON THIS TOPIC

⇒ Talimogene laherparepvec (T-VEC) is the first oncolytic virus approved for the treatment of melanoma where it has a 31.5% objective response rate. T-VEC has been evaluated in combination with immune checkpoint blockade and radiation therapy demonstrating improved therapeutic activity in patients with melanoma and in murine tumor models, although the mechanism(s) underlying this antitumor immunity is/are unclear.

WHAT THIS STUDY ADDS

⇒ Combination of a murine-adapted T-VEC and radiation therapy enhanced therapeutic responses were dependent on IL-1α and induced high expression of PD-L1. Triple treatment with mT-VEC, radiation, and PD-1 blockade was used to drive further therapeutic activity and resulted in a nearly complete response in a patient with anti-PD-1-refractory advanced squamous cell carcinoma.

HOW THIS STUDY MIGHT AFFECT RESEARCH, PRACTICE OR POLICY

⇒ Further clinical studies of combination oncolytic viruses with radiation therapy and immune checkpoint blockade are warranted. IL-1α may be an important mediator of antitumor immunity and merits further investigation as a target for cancer immunotherapy.

BACKGROUND

Immunotherapy, most notably with immune checkpoint inhibition, has improved clinical outcomes for a growing number of different tumor types. Primary and acquired drug resistance, however, often impede clinical benefit. Therefore, new strategies that overcome resistance are a high priority for clinical development. Other cancer therapeutics, including

cytotoxic chemotherapy, targeted therapy, oncolytic viruses (OVs), and radiation therapy (RT), are known to influence immune responses in patients with cancer. Further, these modalities typically have non-overlapping toxicity profiles. Therefore, multiple combination approaches have been proposed for overcoming immune checkpoint inhibitor (ICI) resistance. We report a case in which a patient with anti-PD-1-refractory metastatic cutaneous squamous cell carcinoma (cSCC) was treated with triple combination talimogene laherparepvec (T-VEC; a modified Herpes simplex, type 1 OV), external beam RT, and nivolumab. This patient achieved durable tumor control, and in a surrogate animal model, we further demonstrated the mechanism of the therapeutic response.

METHODS

Cell culture

UACC-257 human melanoma cell line (NCI) and B16-F10-nectin murine melanoma cell line (Amgen) were cultured in Dulbecco's Modified Eagle's Medium (Gibco) supplemented with 10% fetal bovine serum (Sigma) and penicillin/streptomycin (Sigma) at 37°C in a 5% CO_2 humidified incubator. Cells were grown until approximately 70% confluence in culture flasks and passaged similarly once if needed to produce adequate tumor cell numbers. Cells were detached using 0.25% trypsin EDTA (Corning) for passaging or use, as per manufacturer instructions.

3-(4,5-dimethylthiazol-2-yl)–2,5-diphenyltetrazolium bromide cell viability assay

Cells were cultured in 24-well plates to reach 50% confluence (day 0) before subjecting cells to either T-VEC (Amgen), RT, or both. Specifically, on day 1, cells were incubated with T-VEC at various multiplicities of infection (0, 0.01, 0.1 or 1). On day 2, cells were treated with 8 Gy (UACC-257) or 2 Gy (B16-F10-nectin) radiation using a Gamma Cell 40 Exactor (MDS Nordion) irradiator. The Gammacell 40 Exactor Low Dose Rate Research Irradiator uses two Caesium-137 sources which deliver photons with an energy of 0.6617 MeV at a central dose rate of 1.0 Gy/minute. At 48 hours post-treatment, 3-(4,5-dimethylthiazol-2-yl)−2,5-diphenyltetrazolium bromide (Sigma) was added to cells (final concentration 0.5 mg/mL) and incubated at 37°C for 4 hours. Resulting crystals were dissolved in DMSO and analyzed in a fluorescent plate reader (Tecan Infinite) at a wavelength of 570 nm.

Murine syngeneic B16 melanoma model

C57BL/6 (B6) mice were purchased from The Jackson Laboratory at 6 weeks of age. Mice were housed in specific-pathogen-free facilities and all experiments were conducted in accordance with procedures approved by the Institutional Animal Care and Use Committee (IACUC; 16–025) at Rutgers, The State University of New Jersey. To generate the B16 murine tumor model, B6 mice at 8–10 weeks of age were challenged with B16-F10-nectin cells (100,000) via intradermal injection on the right or both flanks. Primary tumor growth was monitored by Vernier caliper measurements in two perpendicular directions serially (typically, every 2–3 days) after tumor challenge. Treatment of mice was initiated when the tumors reached a size of 3 mm×3 mm to 5 mm×5 mm. For survival experiments, Kaplan-Meier curves were used to calculate survival. As per IACUC protocols, mice were euthanized before tumors reached 400 mm^2 or when a time point for dissection of the mice was reached (typically, when tumor growth curves of the treatment groups were different from the control group/s with statistical significance).

In vivo RT+OncoVEC^{mGMCSF}(mT-VEC) treatments

B6 mice were challenged with B16-F10-nectin cells to the right flank intradermally on day 0. For T-VEC treatment, OncoVEC^{mGMCSF} (mT-VEC; 1×10^6 pfu, Amgen) or mock treatment (PBS buffer) was injected intratumorally on days 6, 10, and 12, or as shown in the experimental design panels. For flank tumor irradiation, mice were anesthetized with intraperitoneal injection of Ketamine (100 mg/kg) and Xylazine (10 mg/kg) and irradiated to the flank tumors to 6 Gy in a Gamma Cell 40 Exactor (MDS Nordion) irradiator on day 10, or as shown in the experimental design panels. Collimation was achieved through 3-cm diameter holes in upper and lower lead shields. The tumor-bearing flank was centered over these holes and the rest of the mouse was positioned above and below lead shielding. For the bilateral flank tumor model, B6 mice were challenged with B16-F10-nectin cells on both flanks intradermally on day 0, and OncoVEC^{mGMCSF} (mT-VEC) and RT treatments were only given to the right flank tumors, as described above. Responders were identified as mice whose tumor-treated growth curves were below those of the control treatment, while non-responders were identified as mice whose tumor-treated growth curves were above those of the control treatment.

In vivo antibody-mediated treatments and depletions

For triple combination studies, B6 mice were challenged with B16-F10-nectin cells to the right flank intradermally on day 0 and treated withOncoVEC^{mGMCSF} (mT-VEC; 1×10^6 pfu) or mock (PBS buffer) intratumorally on days 8, 10, and 14, irradiated the flank tumors to 6 Gy in a Gamma Cell 40 Exactor (MDS Nordion) irradiator on day 10, and intraperitoneal injection of 250 µg of anti-PD-L1 antibody (BioXCell, clone 10F.9G2) or its respective isotype control antibody diluted in InVivoPure pH 6.5 Dilution Buffer (BioXCell) on days 8, 10, 14, 17, and 21. For CD8-depletion and IL-1α-depletion experiments, B6 mice were challenged with B16-F10-nectin cells to the right flanks intradermally on day 0 and treated with OncoVEC^{mGMCSF} (mT-VEC; 1×10^6 pfu) or mock (phosphate-buffered saline *PBS)) intratumorally on days 9, 13, and 15, and irradiated the flank tumors to 6 Gy in a Gamma Cell 40 Exactor (MDS Nordion)

irradiator, as described previously, on day 13. Antibody-mediated CD8 depletions were performed using αCD8 antibody (BioXCell, clone 2.43) or its respective isotype control antibody, which were diluted to desired concentrations in InVivoPure pH 6.5 Dilution Buffer (BioXCell) and administered 250 µg via intraperitoneal injection on days 8, 9, 15, and 22. Antibody-mediated IL-1α depletions were performed using α IL-1α antibody (BioXCell, clone ALF-161) or its respective isotype control antibody, which were diluted to desired concentrations in InVivoPure pH 7.0 Dilution Buffer (BioXCell) and administered 250 µg via intraperitoneal injection on days 8 and 9.

In vivo intratumoral treatment with IL-1α recombinant protein

B6 mice were challenged with B16-F10-nectin cells to the right flanks intradermally on day 0 and treated with OncoVEC^{mGMCSF} (mT-VEC; 1×10^6 pfu) or mock (PBS buffer) intratumorally on days 8, 10, and 14, flanks were irradiated to 6 Gy in a Gamma Cell 40 Exactor (MDS Nordion) irradiator, as described previously, on day 10, and intratumoral injection of 1 µg recombinant IL-1α (BioLegend) prepared in sterile buffer (10 mM NaH_2PO_4, 150 mM NaCl, pH 7.2) was administered on days 7, 8, 10, and 14.

Tissue processing and flow cytometry

Treated flank tumors were resected and mechanically dissociated in C tubes (Miltenyi) using a gentleMACS Octo Dissociator (Miltenyi), using program Tumor 01_01, incubated with 1 mg/mL type IV collagenase from *Clostridium histolyticum* (Sigma-Aldrich) and 10 U/mL DNase I (Promega) at 37°C for 30 min with rocking, then mechanically dissociated again using Dissociator (program Tumor 02_01), followed by applying the dissociated cells through a 40 µm filter and washed with PBS to yield a single-cell suspension. For intratumoral leucocyte determination, extracellular staining was performed using CD45 antibody (BioLegend mouse CD45 antibody, clone 30-F11) in PBS for 30 min at room temperature. LIVE/DEAD Fixable Aqua Dead Cell Stain Kit was used to stain dead cells. Cells were then washed and fixed using Stabilizing Fixative (BD Biosciences). Flow cytometry was performed using a BD LSR II cytometer, and the resulting data were analyzed with FlowJo (TreeStar, V.10.4). Data shown have undergone gating on live singlet lymphocytes using forward scatter and side scatter height, area, and width, as well as LIVE/DEAD, as previously described.[1] For antigen-specific CD8+ T cell determination, tumor samples were stained with a fluorochrome-conjugated major histocompatibility complex (MHC-I) Dextramer for murine gp100 (KVPRNQDWL, Immudex) at a concentration of 5 µL/dextramer in a total volume of 50 µL PBS for 45 min at 4°C, followed by extracellular staining including CD8 antibody (BioLegend anti-mouse CD8a antibody, clone 53–6.7) for 30 min at room temperature.

Immunohistochemistry

Treated tumors were dissected on day 26 and fixed in 10% formalin for 24 hours, embedded in paraffin, and 5 µm sections were prepared on microscope slides. Sections were deparaffinized using Xylene, followed by gradual rehydration with 100%, 90% and 70% ethanol, and rehydrated with PBS buffer. Sections were subjected to primary antibody incubation with CD8a antibody (Thermo Fisher, clone 4SM15) and FoxP3 antibody, followed by incubation with secondary antibody HRP anti-rat IgG (Vector Lab).

T cell receptor sequencing and analysis

Treated flank tumors were dissected and frozen at −80°C. Samples were analyzed using the immunoSEQ assay by Adaptive Biotechnologies to assess the diversity and clonality of the CDR3 region of the T cell receptors (TCRs). Sequences were determined by using a multiplex PCR strategy followed by Illumina sequencing, and the resulting data were analyzed using the immunoSEQ Analyzer software. Neoantigen sequences were defined as TCR sequences in the mTVEC, RT, and mTVEC+RT groups that were not found in the B16 control group or the TVEC skin group (no tumor). B16 (thus, antitumor) TCRs were defined as TCRs that were found in the B16 control group that were also not found in the TVEC skin group (no tumor). To arrive at the chart, the neoantigen TCRs per mouse was divided by the number of B16 antitumor TCRs.

NanoString

Dissected tumors were stored in 1 mL of TRIzol (Invitrogen) at −80°C until RNA extraction was performed. Subsequently, tissues were homogenized using the BEADBUG 6 Microtube Homogenizer (Benchmark). RNA was isolated using the RNeasy Plus Mini Kit (Qiagen). The purity of the resulting RNA was measured using a NanoDrop spectrophotometer (Thermo Fisher Scientific). Profiling of transcripts implicated in the antitumor immune response was assessed via the NanoString PanCancer Immune Profiling Panel using an nCounter Digital Analyzer (NanoString Technologies). Total RNA (100 ng) was used for each sample analyzed, hybridized with 3' biotinylated capture probe and a 5' reporter probe tagged with a fluorescent barcode, and were run on the NanoString nCounter preparation station using the recommended manufacturer protocol. Analysis of NanoString data was performed using the nSolver Analysis software and the nCounter Advanced Analysis module. For gene expression analysis, data were normalized using the geometric mean of a selection of housekeeping genes. Within the related figures, one representative sample (of two analyzed with similar results) is shown per the respective groups.

LegendPlex analysis

Treated flank tumors were resected and mechanically homogenized using a gentleMACS Octo Dissociator

(Miltenyi) and M tubes (with a 600 um mesh preinserted in the tube) in PBS to generate a tissue homogenate (100 mg tumor tissue in 1 mL PBS). Homogenate samples were diluted twofold in assay buffer per the LegendPlex Mouse Cytokine Panel 2 kit (BioLegend) and the assay performed in accordance with the manufacturer's protocol. Data acquisition was performed using a BD LSR II cytometer, and LegendPlex Data Analysis Software was used to determine the cytokine concentrations in the tumor homogenates, as per manufacturer instructions.

RESULTS

Combination OV and RT augments immunogenic cell death and inhibits tumor growth

While combinations of OV (T-VEC) and ICI and combinations of RT and ICI have been previously explored and shown to improve antitumor responses compared with the respective monotherapies,[2] similar studies with OV and RT have been lacking. We first evaluated the combination T-VEC (or a murine-adapted T-VEC, hereafter referred to as OncoVEC^{mGMCSF} or mT-VEC) and RT in human and mouse melanoma cells. We found that combination treatment enhanced melanoma cell death in vitro (figure 1A–C) and significantly inhibited tumor growth in vivo (figure 1D–F). Therapeutic responses were associated with an increase in tumor-infiltrating CD45+ immune cells (figure 1G,H), a concomitant increase in CD8+ T cells (and decrease in T regulatory cells) (figure 1I–J), and an increase in tumor-specific CD8+ T cells (figure 1K). The breadth of CD8+ T cell neoantigen response was greatest with combination OncoVEC^{mGMCSF} and RT (figure 1L), and depletion of CD8+ T cells completely abrogated tumor regression, establishing their role in mediating antitumor activity of OncoVEC^{mGMCSF} and RT (figure 1M,N).

Combination OV and RT induces systemic antitumor immunity

Using a panel of immune-related genes, a conversion of tumors from immunologically 'cold' to 'hot' was observed with combination OncoVEC^{mGMCSF} and RT (figure 1O–Q). Specifically, the complete Nanostring gene panel heatmap demonstrated that the OncoVECmGMCSF (mT-VEC) and RT group exhibited high expression of select genes (red) that incorporate genes from OncoVECmGMCSF (mT-VEC) alone and RT alone, as well as unique genes not expressed at high levels by either single treatment or the control (figure 1O). Further, we analyzed the data using a Nanostring gene panel heatmap with inflammatory genes whose high expression has previously been shown to correlate with improved patient outcomes (figure 1P). Importantly, here, we observed high expression of immune checkpoint, PD-L1 (CD274), but low expression of Lag3. A Nanostring gene panel heatmap with a unique set of genes highly expressed in the OncoVECmGMCSF (mT-VEC) and RT treatment group showed upregulation of proteosome subunits, including psmb10, and MHC genes forming the H2 complex, including H2-D1 and H2-K1 (figure 1Q). Next, based on the importance of raising an immune response that can also reduce untreated distant tumor growth, we examined whether combination OncoVEC^{mGMCSF} and RT produces systemic antitumor effects. In addition to reduction in the primary (treated) tumor (figure 2A,B), a dual-flank tumor model exhibited reduced distant (untreated) tumor growth in a majority of mice, particularly in treatment responders vs untreated controls (figure 2C and online supplemental figure S1), demonstrating that this combination can elicit systemic antitumor activity. Here, it is imperative to note that when all the treated mice were included in the analysis, there appeared to be no systemic effect (online supplemental figure S1D). However, under additional analysis, it became obvious that two outliers hid the clear antitumor effect observed in the remaining six of eight mice (online supplemental figure S1E-F). Further, responders and progressors differed in gene expression (online supplemental figure S1G-I), with progressors resembling controls across a variety of immune markers (online supplemental figure S1I). Importantly, a cytokine multiplex revealed IL-1α as a major player in this combination treatment (figure 2D and online supplemental figure S2) and flow cytometry analysis revealed an increase in IL-1α receptor on immune cells within the tumor microenvironment (figure 2E). Furthermore, depletion of IL-1α significantly reduced the therapeutic effect of the combination therapy (figure 2F,G) and the gene panels resembled that of the untreated control (online supplemental figure S3A-C), while intratumoral administration of recombinant stimulatory IL-1α recapitulated the antitumor effect of combination OncoVEC^{mGMCSF} and RT (online supplemental figure S4), suggesting that combination therapy-induced tumor regression is IL-1α-dependent.

Triple combination of OV and RT with checkpoint blockade further reduces tumor growth and prolongs host survival

Given that gene expression profiling revealed that PD-L1 (CD274) was upregulated with combination treatment (figure 1P, online supplemental figure S1H, and figure S3B) and that the PD-1/PD-L1 axis acts to provide negative feedback in antitumor immune responses, we examined whether addition of a PD-L1 ICI would further enhance therapeutic effects. Importantly, treatment with PD-L1 antibody alone had no effect on tumor growth, demonstrating that in this context the tumor was resistant to ICI therapy (figure 2H–J). However, even though the combination of OncoVEC^{mGMCSF} and RT already achieved potent antitumor effects, the addition of PD-L1 blockade antibody further reduced tumor growth (figure 2I) and prolonged host survival (figure 2J). Additionally, the immune-related genes panel showed greater expression of proimmune (antitumor) products (figure 2K–M), correlating to the in vivo demonstrated reduced tumor growth and prolonged host survival. Specifically, in the triple combination therapy, there was a high level of expression of genes (compared with the other groups)

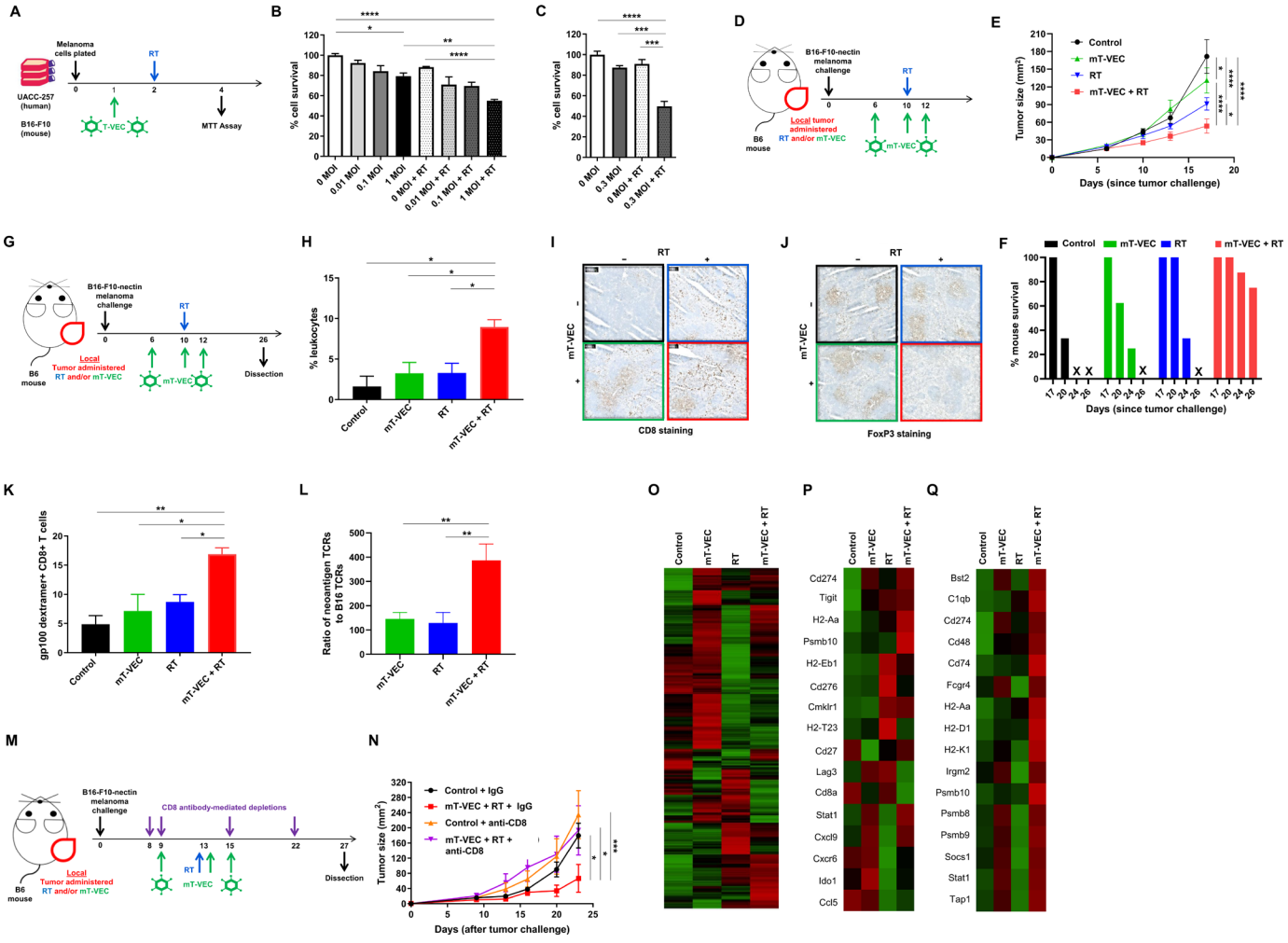

Figure 1 Combination oncolytic virus and radiation therapy (RT) augments melanoma cell death, inhibits tumor growth, and exhibits a unique tumor-infiltrating cell and gene expression profile. (A) Tumor killing assay (in vitro) experimental design. (B) Viral dose-dependent decrease in tumor cell survival of human melanoma cell line, UACC-257, with combination OV (T-VEC; at MOIs shown) and (RT; 8 Gy). Representative graph of one experiment of four conducted in triplicate with similar results. (C) Reduced tumor cell survival of mouse melanoma cell line, B16-F10, with combination OncoVEC^{mGMCSF} (mT-VEC; at dose shown) and RT (2 Gy). Representative graph of one experiment of two conducted in triplicate with similar results. (D) Experimental design for in vivo combination OncoVEC^{mGMCSF} (mT-VEC; 1×10^6 pfu) and RT (6 Gy). (E) Greatest tumor growth reduction with combination OncoVEC^{mGMCSF} (mT-VEC) and RT compared with either treatment alone or compared with PBS control (n=6–8 mice/group). (F) Greatest % mouse survival with combination OncoVEC^{mGMCSF} (mT-VEC) and RT compared with either treatment alone or PBS control (n=6–8 mice/group). (G) Experiment design (in vivo) for combination OncoVEC^{mGMCSF} (mT-VEC) and RT, including designation of the dissection day. (H) Per cent of immune infiltration (CD45+ cells; leucocytes) among all singlet live cells in the tumor at day 26, with greatest % leucocytes in the combination OncoVEC^{mGMCSF} (mT-VEC) and RT group. (n=4–7 mice/group). (I) Representative immunohistochemistry images of CD8+ cells within the tumor, with the greatest staining in the OncoVEC^{mGMCSF} (mT-VEC) and RT group. (J) Immunohistochemistry images of FoxP3+ (regulatory/suppressive) cells within the tumor, with the least staining in the OncoVEC^{mGMCSF} (mT-VEC) and RT group. (K) Bar graph showing greatest % of gp100 dextramer (ie, melanoma tumor-specific) CD8+ T cells in the combination OncoVEC^{mGMCSF} (mT-VEC) and RT group. (n=4–7 mice/group). (L) Bar graph showing the greatest breadth of CD8+ T cell neoantigen response in the combination OncoVEC^{mGMCSF} (mT-VEC) and RT group, using TCR sequencing and calculating the ratio of neoantigen TCRs to B16 antigen TCRs. (n=4–5 mice/group). (M) Experimental design (in vivo) for antibody-mediated CD8 depletion in the context of combination OncoVEC^{mGMCSF} (mT-VEC) and RT treatment of B16–F10 melanoma. (N) Abrogation of the tumor growth reduction of combination OncoVEC^{mGMCSF} (mT-VEC) and RT treatment by CD8 antibody-mediated cell depletion. (n=4–6 mice/group). (O) Nanostring gene panel heatmap, with the OncoVEC^{mGMCSF} (mT-VEC) and RT group exhibiting high expression of select genes (red) that incorporate genes from OncoVEC^{mGMCSF} (mT-VEC) alone and RT alone, as well as unique genes not expressed at high levels by either single treatment or the control. (P) Nanostring gene panel heatmap, with inflammatory genes whose high expression has previously been shown to correlate with improved patient outcomes. (Q) Nanostring gene panel heatmap with a unique set of genes highly expressed in the OncoVEC^{mGMCSF} (mT-VEC) and RT treatment group. All error bars shown are SEM. Statistical significance assessment was performed using one-way ANOVA with Tukey correction for multiple comparisons (B, C, H, K, and L) and two-way ANOVA with Tukey correction for multiple comparisons (E and N). *p<0.05, **p<0.01, ***p<0.001, ****p<0.0001. ANOVA, analysis of variance; MOIs, multiplicities of infection; OV, oncolytic virus; T-VEC, Talimogene laherparepvec.

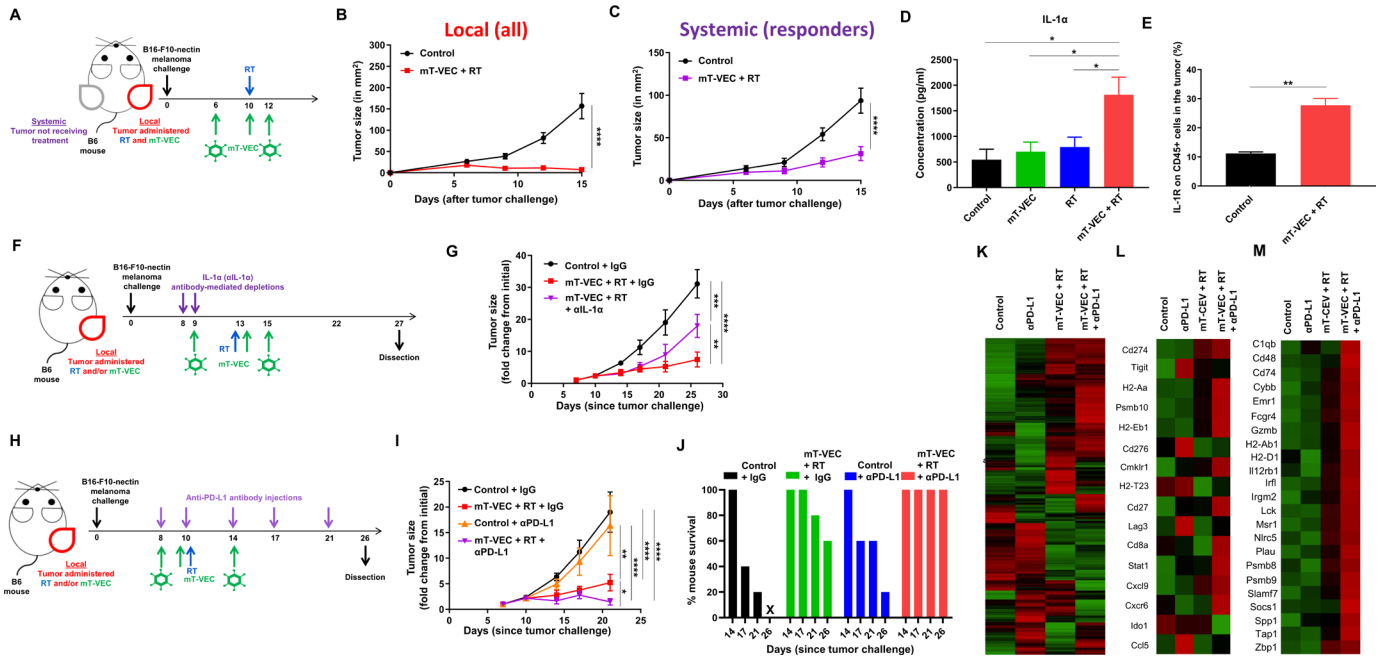

Figure 2 Combination oncolytic virus and radiation therapy (RT) augments PD-1/PD-L1 Blockade and induces abscopal responses. (A) Dual-flank in vivo experimental design for combination OncoVEC^{mGMCSF} (mT-VEC) and RT. (B) Greatest tumor (B16–F10) growth reduction of the primary (right flank) tumor treated with combination OncoVEC^{mGMCSF} (mT-VEC) and RT compared with control (PBS) treatment. (n=6–8 mice/group). (C) Greatest systemic tumor growth reduction of the distant (left flank) untreated tumor in the OncoVEC^{mGMCSF} (mT-VEC) and RT group compared with the control (PBS) treatment (with treatment non-responders removed, as per online supplemental figure S1). (n=6–8 mice/group). (D) Greatest production of intratumoral (B16–F10) IL-1α in the OncoVECmGMCSF (mT-VEC) and RT group compared with the single treatments and control (PBS) treatment. (n=5–7 mice/group). (E) Increased expression of IL-1α receptor (IL-1α R) on CD45+ (leucocytes) within the tumor microenvironment with combination OncoVECmGMCSF (mT-VEC) and RT treatment. (F) Experimental design (in vivo) for determining the role of IL-1α in combination OncoVEC^{mGMCSF} (mT-VEC) and RT tumor (B16-F10 melanoma) reduction capability. (G) Cumulative tumor growth curve with antibody-mediated depletion of IL-1α, with IL-1α depletion partially abrogating the ability of combination OncoVEC^{mGMCSF} (mT-VEC) and RT to reduce tumor growth. (H) Experimental design (in vivo) for triple combination OncoVEC^{mGMCSF} (mT-VEC), RT, and αPD-L1. (I) Greatest tumor growth (B16–F10) reduction with triple combination OncoVEC^{mGMCSF} (mT-VEC), RT, and αPD-L1 treatment. (J) Greatest % mouse survival with triple combination OncoVEC^{mGMCSF} (mT-VEC), RT, and αPD-L1. (K) Nanostring gene panel heatmap, with the OncoVEC^{mGMCSF} (mT-VEC), RT, αPD-L1 group exhibiting high expression of select genes (red) that incorporate genes from αPD-L1 alone and OncoVEC^{mGMCSF} (mT-VEC) and RT combination, as well as unique genes not expressed at high levels by either treatment group or the control. (L) Nanostring gene panel heatmap, with inflammatory genes whose high expression has previously been shown to correlate with improved patient outcomes. (M) Nanostring gene panel heatmap with a unique set of genes highly expressed in the triple combination OncoVEC^{mGMCSF} (mT-VEC), RT, and αPD-L1 treatment group. All error bars shown are SEM. Statistical significance assessment was performed using two-way ANOVA with Bonferroni correction for multiple comparisons (B, F), one-way ANOVA with Bonferroni correctio for multiple comparisons (D). *p<0.05, **p<0.01, ***p<0.001, ****p<0.0001. ANOVA, analysis of variance; T-VEC, talimogene laherparepvec.

associated with positive antitumor response, including those associated with costimulatory molecule, CD27, proteosome subunit, Psmb10, MHC gene forming the H2 complex, H2-D1, and cytolytic molecule GzmB (figure 2L,M).

Triple combination of OV and RT with ICI leads to tumor regression and prolonged patient survival

Currently, no indication exists for the utilization of the combination OV, RT, and ICI, and clinical trials designs for such clinical trials are complex. We do report a single case of a patient in his late 60s who presented in May 2017 with a cSCC of the right postauricular scalp and approximately five pulmonary nodules concerning for metastases. He underwent a right lower lobe wedge resection, and pathology demonstrated a 1.6 cm SCC metastasis. He enrolled on a clinical trial of cemiplimab. He initially had a partial response to therapy, but after 10 months the postauricular tumor grew and he was removed from study due to progressive disease. In May 2018, he enrolled in an NCI-sponsored trial (NCT02978625) of T-VEC followed by combination T-VEC and nivolumab (figure 3). During the initial T-VEC lead-in, the ulcerating, fungating postauricular tumor grew from 6 cm to 9.5 cm, and a new 7 mm right upper lobe nodule was seen on a CT scan of the chest in July 2018, which quickly grew to 16 mm in August 2018. In August 2018, he had significant tumor-related pain and underwent a course of palliative RT (50 Gy in 20 fractions), completed in October 2018. T-VEC was

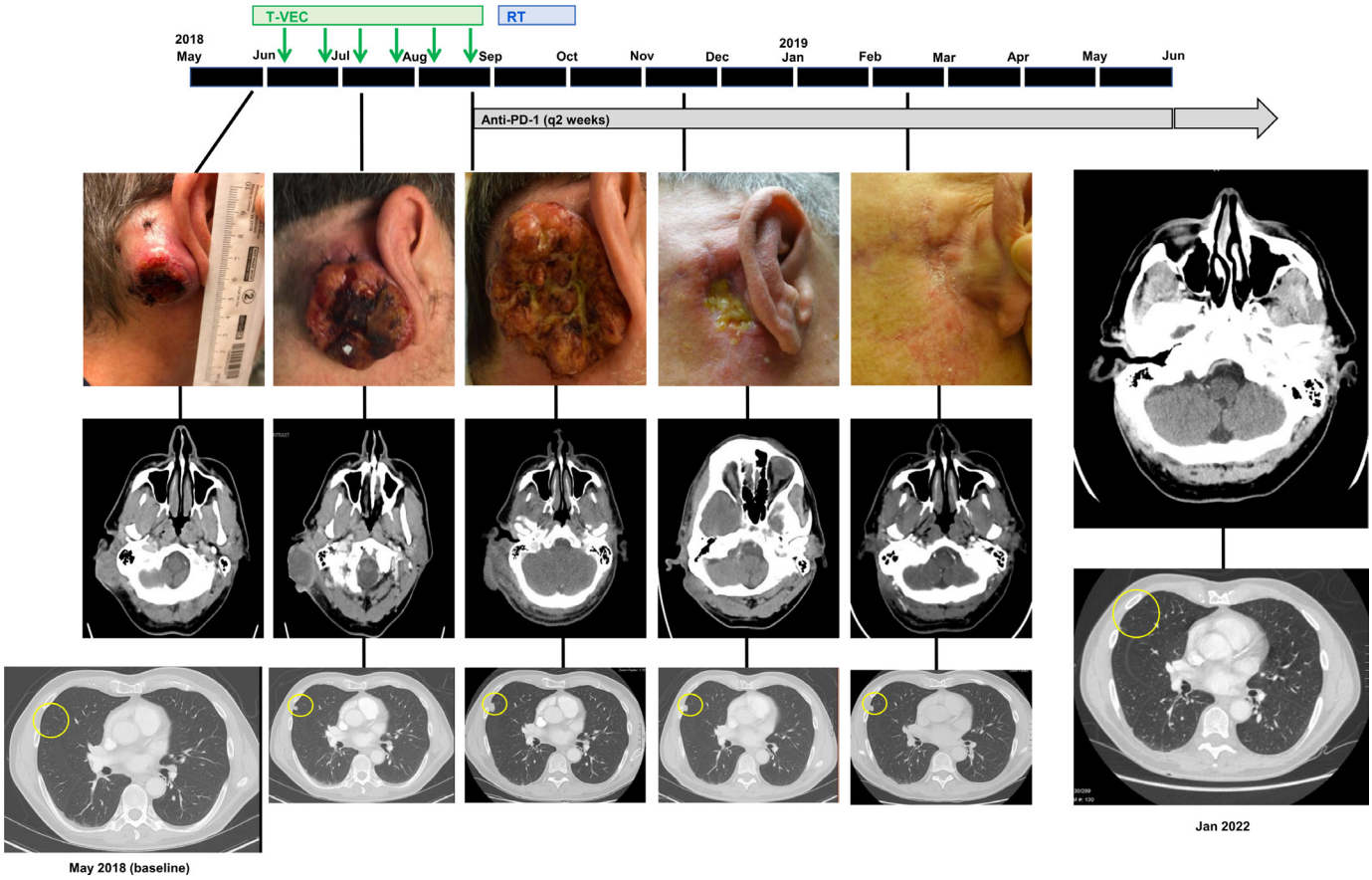

Figure 3 A case of skin cancer responsive to triple combination treatment of oncolytic virus (OV), immune checkpoint inhibitor (ICI), and radiation therapy (RT). Clinical course and treatment timeline of the patient. (Upper images) photographs of the tumor progression until addition of palliative RT in October 2018 to previous OV (T-VEC) and ICI, nivolumab (αPD-1). (Lower images) Axial CT of subcutaneous squamous cell carcinoma and CT images of the pulmonary metastasis accompanying the photographs. The CT images on the right show near complete resolution of tumors more than 44 months after study entry.

held during RT and then discontinued because the tumor had involuted and there was no longer an injectable lesion present. The patient continued on nivolumab after completion of his radiation course and in February of 2019 was noted to have a near-complete clinical and radiographic response in the primary site with a slight decrease in lung nodules. He continued nivolumab until June 2020 without significant adverse events. He has been observed off treatment and remains without evidence of progression more than 44 months since study entry. His surveillance scans show only thickening of the postauricular skin and improving small indeterminate pulmonary opacities, consistent with scars from prior surgery and previous sites of pulmonary metastases.

DISCUSSION/CONCLUSIONS

Here, we report an unexpected outcome of long-term disease control in metastatic skin cancer treated with combination OV (T-VEC), RT, and ICI (αPD-L1) after progression on αPD-L1. Although it is possible that the clinical response was due to radiation alone, the regression of distant pulmonary metastases that did not receive radiation suggests an interaction between all three modalities. Further, the patient did not exhibit any unexpected toxicity, tolerating all treatments well, suggesting that triple combination of OV, RT and checkpoint blockade may be worthy of further clinical investigation. This may be particularly true since these therapeutics are currently available and are especially timely for neoadjuvant therapy which recently has emerged as a new important area for considering immunotherapy-based treatments in cSCC.[3]

To better understand the underlying molecular and cellular mechanisms of the clinical effects, we sought to replicate the triple combination therapy in preclinical models. Specifically, we demonstrated that while monotherapy OV and RT treatments reduce cell line and mouse tumor growth to a limited degree, the combination results in significantly greater tumor growth reduction and prolonged host survival. In our model, this is mediated by IL-1α and improved antitumor CD8+ T cell responses, as demonstrated by immune cell depletion studies, gene expression profiling, and IHC. This is consistent with previous evidence that CD8+ T cell-mediated cytotoxicity is integral in the antitumor response induced by RT or OVs, individually.[4–9] A potential drawback to OV and RT

treatment, however, is the induction of counterregulatory checkpoint (PD-L1) expression within the tumor. This potential inhibition of immune responses was addressed by the addition of ICI treatment, ultimately comprizing an effective triple combination therapy. Combinations of various ICIs and RT have previously demonstrated improved local tumor control and systemic disease responses in murine tumor models.[9–12]

We also found that intratumoral IL-1α contributes to the therapeutic efficacy of combination OV and RT therapy. IL-1α is an inflammatory cytokine of the IL-1 family that exerts its function through binding of IL-1R1 (IL-1αR). IL-1α functions are multifaceted, and IL-1α can act as an extracellular cytokine, an intracellular transcriptional coactivator, or a membrane-bound ligand in immune and non-immune cell types.[13] Release of intracellular IL-1α from necrotic cells acts as an alarmin or DAMP to trigger inflammation.[14] In addition, expression of membrane-associated IL-1α in tumor cells has been shown to induce antitumor immunity, which results in reduced tumor invasiveness and tumor regression.[15–18] In line with these studies, our work suggests that antibody depletion of extracellular IL-1α results in an attenuation of the tumoricidal effect of combined therapy, while intratumoral injection of recombinant IL-1α significantly inhibits tumor growth. While elucidating the mechanism behind the IL-1α antitumor effect is beyond the scope of this study, we hypothesize that increased IL-1α expression in the intratumoral milieu, through IL-1R1 binding, contributes to a short (stimulatory) burst of inflammation which results in antitumor immune activation. A complete loss of tumor killing after IL-1α depletion was neither observed nor expected, due to the additional intrinsic cytotoxic effects of combination OV and RT.

We also demonstrated an abscopal effect using combination OncoVEC^{mGMCSF}+RT therapy in a bilateral flank tumor model. Intriguingly, to date, this effect remains a rare entity in the clinic, and in line with this, we identified two distinct cohorts—abscopal responders and progressors (non-responders) to this combination therapy. Gene profiling revealed immune activation in responders compared with progressors, but interestingly, also demonstrated distinct immune-related gene expression in progressors compared with untreated tumors. Our findings mimic what is commonly observed in clinic, in which tumors of the same type exhibit widely varying responses to immunotherapy in different patients.[19] Even in the context of identical tumor genetic backgrounds, environmental differences and epigenetic modulation may influence immune surveillance processes, tumor mutational burden, overall immunogenicity, and responses to treatment,[20] and is therefore, an important subject of future studies. We also provided an example of one patient with ICI-refractory cancer who achieved a clinical benefit with combination therapy. While this is a single anecdotal case report, it provides an approach for how triple combination treatment could be integrated into clinical care and may pave the way for future clinical trial designs to further validate this approach.

In summary, our study demonstrates therapeutic synergy with combination OV, RT, and ICI treatment in the clinical and preclinical context of cutaneous malignancies. These effects induced durable response in a patient with an ICI-refractory metastatic cSCC. In a preclinical surrogate model, the therapeutic activity was dependent on IL-1α and recruitment of CD8+ T cells. Overall, our data provide strong rationale for combining OV, RT, and ICI for treatment of patients with ICI-refractory skin and potentially other cancers.

Author affiliations
[1]Department of Radiation Oncology, The Ohio State University Wexner Medical Center, Columbus, Ohio, USA
[2]Department of Orthopedic Surgery, Allegheny Health Network, Pittsburgh, Pennsylvania, USA
[3]Rutgers Cancer Institute of New Jersey, Rutgers, The State University of New Jersey, New Brunswick, New Jersey, USA
[4]Department of Internal Medicine, Rush University Medical Center, Chicago, Illinois, USA
[5]Harvard Medical School, Boston, Massachusetts, USA
[6]Department of Dermatology, Brigham and Women's Hospital, Boston, Massachusetts, USA
[7]Department of Medical Oncology, Dana-Farber Cancer Institute, Boston, Massachusetts, USA
[8]Department of Radiology, The George Washington University School of Medicine and Health Sciences, Washington, District of Columbia, USA
[9]Department of Pharmacology and Toxicology, Ernest School of Pharmacy, Rutgers, The State University of New Jersey, Piscataway, New Jersey, USA
[10]Department of Immunology, Moffitt Cancer Center, Tampa, Florida, USA
[11]Department of Surgery, Massachusetts General Hospital, Boston, Massachusetts, USA

Correction notice This article has been corrected since it was first published online. The author Eileena F Giurini was omitted from the author list. This has now been amended.

Acknowledgements The B16-F10-nectin murine melanoma cell line and murine-adapted T-VEC (OncoVECmGMCSF; mT-VEC) were kindly provided by Amgen, Inc.

Contributors SRJ and S-JW: acquisition of the data, analysis of the data, interpretation of the results, manuscript writing. AT, PB, JN and DS: acquisition of the data, analysis of the data, interpretation of the results, review or revision of the manuscript for important intellectual content. ALM, TMK, VG, JR, PD, DM, NRL, CS, SG, AL, JAG-P and BH: review or revision of the manuscript for important intellectual content. HLK: provision of study materials, logistical or technical support, interpretation of the results, and review or revision of the manuscript for important intellectual content. AWS: provision of the patient data, design and planning of studies, analysis of the data, interpretation of the results, manuscript writing, and guarantor. AZ: conception of the studies, design and planning of the studies, supervision of the research, analysis of the data, interpretation of the results, manuscript writing, and guarantor.

Funding This study was funded in part by Amgen, via grant PRPA 2015643490. One Amgen Center Drive, Thousand Oaks, CA, 91320-1799

Competing interests HLK is an employee of Ankyra Therapeutics and has served on advisory boards for Castle Biosciences, Marengo Therapeutics, and Virogin. AWS reports receiving grants/research support (to the Institution) from Biohaven Pharmaceuticals, Replimune, Morphogenesis, Shattuck Laboratories, advisory board fees from InStil Bio and Signatera, and royalties from UpToDate. AZ holds equity in Primevax Immuno-Oncology.

Patient consent for publication Consent obtained directly from patient(s).

Provenance and peer review Not commissioned; externally peer reviewed.

Data availability statement Data are available on reasonable request.

ORCID iDs
Praveen K Bommareddy http://orcid.org/0000-0003-0089-8693
Jose A Guevara-Patino http://orcid.org/0000-0002-6258-7228
Howard L Kaufman http://orcid.org/0000-0003-1131-004X
Ann W Silk http://orcid.org/0000-0003-3877-3984
Andrew Zloza http://orcid.org/0000-0001-8844-6493

REFERENCES

1 Zloza A, Kohlhapp FJ, Lyons GE, *et al*. Nkg2D signaling on Cd8+ T cells represses T-bet and Rescues Cd4-unhelped Cd8+ T cell memory recall but not Effector responses . *Nat Med* 2012;18:422–8.
2 Bommareddy PK, Shettigar M, Kaufman HL. Author correction: integrating Oncolytic viruses in combination cancer Immunotherapy. *Nat Rev Immunol* 2018;18:536.
3 Gross ND, Miller DM, Khushalani NI, *et al*. Neoadjuvant Cemiplimab for stage II to IV cutaneous squamous-cell carcinoma. *N Engl J Med* 2022;387:1557–68.
4 Stone HB, Peters LJ, Milas L. Effect of host immune capability on Radiocurability and subsequent Transplantability of a murine Fibrosarcoma. *J Natl Cancer Inst* 1979;63:1229–35.
5 Lugade AA, Moran JP, Gerber SA, *et al*. Local radiation therapy of B16 Melanoma tumors increases the generation of tumor antigen-specific Effector cells that traffic to the tumor. *J Immunol* 2005;174:7516–23.
6 Apetoh L, Ghiringhelli F, Tesniere A, *et al*. Toll-like receptor 4-dependent contribution of the immune system to anticancer chemotherapy and radiotherapy. *Nat Med* 2007;13:1050–9.
7 Lee Y, Auh SL, Wang Y, *et al*. Therapeutic effects of Ablative radiation on local tumor require Cd8+ T cells: changing strategies for cancer treatment. *Blood* 2009;114:589–95.
8 Golden EB, Apetoh L. Radiotherapy and Immunogenic cell death. *Semin Radiat Oncol* 2015;25:11–7.
9 Zamarin D, Holmgaard RB, Subudhi SK, *et al*. Localized Oncolytic Virotherapy overcomes systemic tumor resistance to immune Checkpoint blockade Immunotherapy. *Sci Transl Med* 2014;6:226ra32.
10 Woller N, Gürlevik E, Fleischmann-Mundt B, *et al*. Viral infection of tumors overcomes resistance to PD-1-Immunotherapy by broadening Neoantigenome-directed T-cell responses. *Mol Ther* 2015;23:1630–40.
11 Liu Z, Ravindranathan R, Kalinski P, *et al*. Rational combination of Oncolytic Vaccinia virus and PD-L1 blockade works synergistically to enhance therapeutic efficacy. *Nat Commun* 2017;8:14754.
12 Saha D, Martuza RL, Rabkin SD. Macrophage polarization contributes to glioblastoma eradication by combination Immunovirotherapy and immune Checkpoint blockade. *Cancer Cell* 2017;32:253–67.
13 Dinarello CA. Immunological and inflammatory functions of the Interleukin-1 family. *Annu Rev Immunol* 2009;27:519–50.
14 Chen CJ, Kono H, Golenbock D, *et al*. Identification of a key pathway required for the sterile inflammatory response triggered by dying cells. *Nat Med* 2007;13:851–6.
15 Marhaba R, Nazarenko I, Knöfler D, *et al*. Opposing effects of Fibrosarcoma cell-derived IL-1 alpha and IL-1 beta on immune response induction. *Int J Cancer* 2008;123:134–45.
16 Zoller M, Douvdevani A, Segal S, *et al*. Interleukin-1 production by transformed fibroblasts. *Int J Cancer* 1992;50:450–7.
17 Voronov E, Weinstein Y, Benharroch D, *et al*. Antitumor and Immunotherapeutic effects of activated invasive T lymphoma cells that display short-term interleukin 1Alpha expression. *Cancer Res* 1999;59:1029–35.
18 Song X, Voronov E, Dvorkin T, *et al*. Differential effects of IL-1 alpha and IL-1 beta on Tumorigenicity patterns and Invasiveness. *J Immunol* 2003;171:6448–56.
19 Fridman WH, Pagès F, Sautès-Fridman C, *et al*. The immune Contexture in human tumours: impact on clinical outcome. *Nat Rev Cancer* 2012;12:298–306.
20 Chatterjee A, Rodger EJ, Eccles MR. Epigenetic drivers of Tumourigenesis and cancer metastasis. *Semin Cancer Biol* 2018;51:149–59.